

Study of $B \rightarrow X(3872)K\pi$ at BelleA. BALA^a, V. BHARDWAJ^{1b}, K. TRABELSI^c, J.B. SINGH^a^a*Department of Physics**Panjab University, Chandigarh 160014, India*^b*Department of Physics and Astronomy**University of South Carolina, Columbia, SC 29208, USA*^c*Institute of Particle and Nuclear Studies (KEK)**Tsukuba, Ibaraki-ken 305-0801, Japan*

We report the first observation of $B^0 \rightarrow X(3872)(K^+\pi^-)$ and evidence for $B^+ \rightarrow X(3872)(K^0\pi^+)$. The product of branching fractions for the former decay mode is measured to be $\mathcal{B}(B^0 \rightarrow X(3872)(K^+\pi^-)) \times \mathcal{B}(X(3872) \rightarrow J/\psi\pi^+\pi^-) = (7.9 \pm 1.3(\text{stat.}) \pm 0.4(\text{syst.})) \times 10^{-6}$ and also find that $B^0 \rightarrow X(3872)K^*(892)^0$ does not dominate the $B^0 \rightarrow X(3872)K^+\pi^-$ decay mode in contrast to other charmonium states like ψ' . The product of branching fractions for the latter decay mode is measured to be $\mathcal{B}(B^+ \rightarrow X(3872)(K^0\pi^+)) \times \mathcal{B}(X(3872) \rightarrow J/\psi\pi^+\pi^-) = (10.6 \pm 3.0(\text{stat.}) \pm 0.9(\text{syst.})) \times 10^{-6}$. This study is based on the full and final data sample of 711 fb^{-1} ($772 \times 10^6 B\bar{B}$ pairs) collected at the $\Upsilon(4S)$ resonance with the Belle detector at the KEKB collider.

PRESENTED AT

The 7th International Workshop on Charm Physics

(CHARM 2015)

Detroit, MI, 18-22 May, 2015

¹Speaker on behalf of Belle Collaboration, supported by U.S. Department of Energy.

1 Introduction

Belle Collaboration discovered the $X(3872)$ state [1] in the exclusive reconstruction of $B^+ \rightarrow X(3872)(\rightarrow J/\psi\pi^+\pi^-)K^+$ [2] about more than a decade ago. Currently, we know precisely its mass (3871.69 ± 0.17) MeV/ c^2 [3], have a stringent limit on its width (less than 1.2 MeV at 90% confidence level) [4] along with definitive J^{PC} assignment of 1^{++} [5]. It has been observed to decay to the following final states: $J/\psi\gamma$ [6], $\psi'\gamma$ [7], $J/\psi\pi^+\pi^-\pi^0$ [8], $J/\psi\pi^+\pi^-$ [1] and $D^0\bar{D}^{*0}$ [9, 10]. Till now, $X(3872)$ has been observed and studied in two body B meson decays. This is the first time, we have observed $X(3872)$ in three body B decay and estimated the product of branching fractions using full and final Belle data set to understand its mysterious nature. In this analysis, we also did the comparison of this exotic state “ $X(3872)$ ” with ordinary charmonium states by considering ψ' as calibration sample.

We present study of $X(3872)$ production via the $B^0 \rightarrow X(3872)K^+\pi^-$ and $B^+ \rightarrow X(3872)K_S^0\pi^+$ decay modes, where the $X(3872)$ decays to $J/\psi\pi^+\pi^-$. The study is based on 711 fb^{-1} of data containing 772×10^6 $B\bar{B}$ events collected with the Belle detector [11] at the KEKB e^+e^- asymmetric-energy collider [12] operating at the $\Upsilon(4S)$ resonance.

2 Selection criterion

To find the reconstruction efficiencies, signal Monte Carlo (MC) samples are generated for each decay mode using EvtGen [13] and radiative effects are taken into account using the PHOTOS [14] package. The detector response is simulated using Geant3 [15]. The selection criteria is same for signal MC events, background MC events and data events for calibration sample (having ψ') and for concerned decay modes (having $X(3872)$) except the difference of $M_{J/\psi\pi^+\pi^-}$ range as both (ψ' and $X(3872)$) are further reconstructed from $J/\psi\pi^+\pi^-$.

We reconstruct J/ψ mesons in the $\ell^+\ell^-$ decay channel ($\ell = e$ or μ) and include bremsstrahlung photons that are within 50 mrad of either the e^+ or e^- tracks [hereinafter denoted as $e^+e^-(\gamma)$]. The invariant mass of the J/ψ candidate is required to satisfy $3.00 \text{ GeV}/c^2 < M_{e^+e^-(\gamma)} < 3.13 \text{ GeV}/c^2$ or $3.06 \text{ GeV}/c^2 < M_{\mu^+\mu^-} < 3.13 \text{ GeV}/c^2$ (with a distinct lower value accounting for the residual bremsstrahlung in the electron mode). The J/ψ candidate is then combined with a $\pi^+\pi^-$ pair to form an $X(3872)$ (ψ') candidate whose mass must satisfy $3.82 \text{ GeV}/c^2 < M_{J/\psi\pi^+\pi^-} < 3.92 \text{ GeV}/c^2$ ($3.64 \text{ GeV}/c^2 < M_{J/\psi\pi^+\pi^-} < 3.74 \text{ GeV}/c^2$). The dipion mass must also satisfy $M_{\pi^+\pi^-} > M_{J/\psi\pi^+\pi^-} - (m_{J/\psi} + 0.2 \text{ GeV}/c^2)$, where $m_{J/\psi}$ is nominal mass. This criterion corresponds to $M_{\pi^+\pi^-} > 575$ (389) MeV/ c^2 for the $X(3872)$ (ψ') mass region and it reduces significantly the combinatorial background [4] with an advantage of flattening the background distribution in $M_{J/\psi\pi^+\pi^-}$. To suppress the background

from continuum events, we require $R_2 < 0.4$, where R_2 is the ratio of the second- to zeroth-order Fox-Wolfram moments [16].

To reconstruct neutral (charged) B meson candidate, a $K^+\pi^-$ ($K_S^0\pi^+$) candidate is further combined with the $X(3872)$ for concerned decay mode and with ψ' for the study of calibration sample. B candidates are selected using two kinematic variables: the energy difference $\Delta E = E_B^* - E_{\text{beam}}$ and the beam-energy constrained mass $M_{\text{bc}} = (\sqrt{E_{\text{beam}}^2 - p_B^{*2}c^2})/c^2$, where E_{beam} is the beam energy and E_B^* and p_B^* are the energy and magnitude of momentum, respectively, of the candidate B -meson, all calculated in the e^+e^- center-of-mass (CM) frame. More details regarding the selection criteria can be found in Ref. [17].

3 Signal Extracton

To extract the signal yield of $B \rightarrow X(3872)(\rightarrow J/\psi\pi^+\pi^-)K\pi$, we perform a two-dimensional (2D) unbinned extended maximum likelihood fit to the ΔE and $M_{J/\psi\pi\pi}$ distributions. The 2D probability distribution function (PDF) is a product of the individual one-dimensional PDFs, as no sizable correlation is found.

In order to study backgrounds, we use a large Monte Carlo sample of $B \rightarrow J/\psi X$ events, corresponds to 100 times the integrated luminosity of the data sample. Based upon above study we find that few backgrounds are peaking in the $M_{J/\psi\pi\pi}$ distribution (nonpeaking in the ΔE distribution) and vice versa. The remaining backgrounds are combinatorial in nature and are flat in both distributions.

For the signal, the ΔE dimension parametrization is done by the sum of a Crystal Ball [18] and a Gaussian function while the $M_{J/\psi\pi\pi}$ distribution is modeled using the sum of two Gaussians having a common mean. The mean and resolution of ΔE and $M_{J/\psi\pi\pi}$ are fixed for the $X(3872)$ mass region from signal MC samples after being rescaled from the results of the $B^0 \rightarrow \psi'K^+\pi^-$ decay mode. Further, we correct the mean of a Gaussian function for the $M_{J/\psi\pi\pi}$ distribution because of difference between the decay dynamics of ψ' and $X(3872)$. The tail parameters are fixed according to the signal MC simulation. The peaking components can be divided into two categories: the one peaking in $M_{J/\psi\pi\pi}$ but non-peaking in ΔE that comes from the $B \rightarrow X(3872)X'$ decays where the $X(3872)$ decays in $J/\psi\pi^+\pi^-$ [here X' can be any particle], and the other peaking in ΔE but non-peaking in $M_{J/\psi\pi\pi}$ which comes from a B with the same final state where $J/\psi\pi^+\pi^-$ is not from a $X(3872)$. The peaking background in ΔE ($M_{J/\psi\pi\pi}$) is found to have the same resolution as that of the signal, so the PDF is chosen to be the same as the signal PDF, while the non-peaking background in the other dimension is parameterized with a first-order Chebyshev polynomial. For the combinatorial background in both dimensions, a first-order Chebyshev polynomial is used. The fits are first validated on full simulated experiments and toy MC studies and no significant bias is seen. Fig. 1 (top) shows

the signal-enhanced projection plots for the $B^0 \rightarrow X(3872)(K^+\pi^-)$ decay mode. The result of the fit and branching fractions derived are listed in Table 1. We observe a clear signal for $B^0 \rightarrow X(3872)K^+\pi^-$ with 116 ± 19 signal events corresponding to a significance (including systematic uncertainties related to the signal yield as mentioned in Table 1) of 7.0 standard deviations (σ), and measure the product of branching fractions to be $\mathcal{B}(B^0 \rightarrow X(3872)K^+\pi^-) \times \mathcal{B}(X(3872) \rightarrow J/\psi\pi^+\pi^-) = (7.9 \pm 1.3(\text{stat.}) \pm 0.4(\text{syst.})) \times 10^{-6}$. The above fit is validated on the calibration

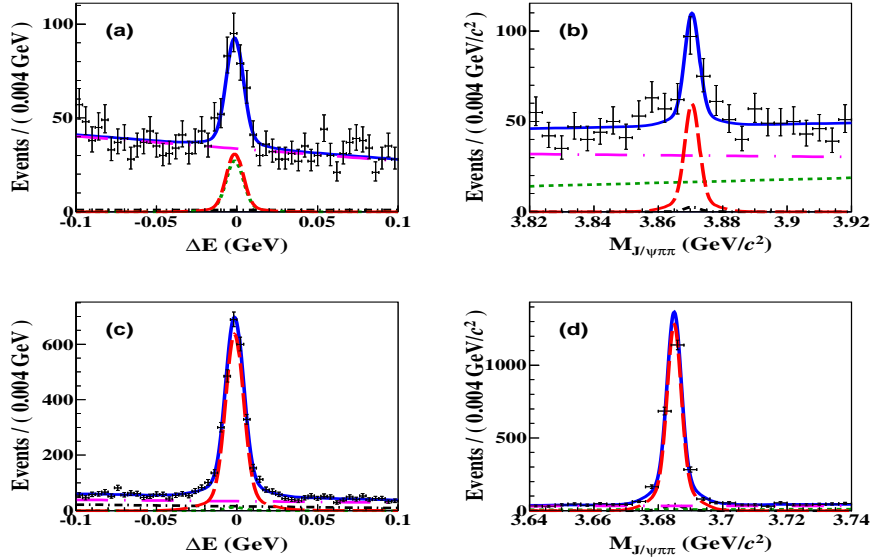


Figure 1: Projections of (a) ΔE distribution with $3.860 \text{ GeV}/c^2 < M_{J/\psi\pi\pi} < 3.881 \text{ GeV}/c^2$, (b) $M_{J/\psi\pi\pi}$ distribution with $-11 \text{ MeV} < \Delta E < 8 \text{ MeV}$, (c) ΔE distribution with $3.675 \text{ GeV}/c^2 < M_{J/\psi\pi\pi} < 3.695 \text{ GeV}/c^2$, and (d) $M_{J/\psi\pi\pi}$ distribution with $-11 \text{ MeV} < \Delta E < 8 \text{ MeV}$ for $B^0 \rightarrow X(3872)(\rightarrow J/\psi\pi^+\pi^-)K^+\pi^-$ decay mode (top) and the $B^0 \rightarrow \psi'(\rightarrow J/\psi\pi^+\pi^-)K^+\pi^-$ decay mode (bottom). The curves show the signal [red long-dashed] and the background components [black dashed-dotted for the component peaking in $M_{J/\psi\pi\pi}$ but non-peaking in ΔE , green dashed for the one peaking in ΔE but non-peaking in $M_{J/\psi\pi\pi}$, and magenta long dashed-dotted for combinatorial background] as well as the overall fit [blue solid].

mode $B^0 \rightarrow \psi'K^+\pi^-$. Fig. 1 (bottom) shows the signal-enhanced projection plots for the $B^0 \rightarrow \psi'(K^+\pi^-)$ decay mode. We measure the branching fraction to be $\mathcal{B}(B^0 \rightarrow \psi'K^+\pi^-) = (5.79 \pm 0.14(\text{stat.})) \times 10^{-4}$, consistent with an independent Belle result based on a Dalitz-plot analysis [19].

Further, to determine the contribution of the $K^*(892)$ and other intermediate states, we perform a 2D fit to ΔE and $M_{J/\psi\pi\pi}$ in each bin of $M_{K\pi}$ (100-MeV wide

Table 1: Signal yield (Y) from the fit, weighted efficiency (ϵ) after PID correction, significance (Σ) and measured \mathcal{B} for $B^0 \rightarrow X(3872)K^+\pi^-$ and $B^+ \rightarrow X(3872)K^0\pi^+$. The first (second) uncertainty represents a statistical (systematic) contribution.

Decay Mode	Yield (Y)	ϵ (%)	Σ (σ)	$\frac{\mathcal{B}(B \rightarrow X(3872)K\pi) \times \mathcal{B}(X(3872) \rightarrow J/\psi\pi^+\pi^-)}{\mathcal{B}(X(3872) \rightarrow J/\psi\pi^+\pi^-)}$
$B^0 \rightarrow X(3872)K^+\pi^-$	116 ± 19	15.99	7.0	$(7.9 \pm 1.3 \pm 0.4) \times 10^{-6}$
$B^+ \rightarrow X(3872)K^0\pi^+$	35 ± 10	10.31	3.7	$(10.6 \pm 3.0 \pm 0.9) \times 10^{-6}$

bins of $M_{K\pi}$ in the range $[0.62, 1.42]$ GeV/ c^2) for $X(3872)$ mass region, which provides a background-subtracted $M_{K\pi}$ signal distribution. All parameters of the signal PDFs for $M_{J/\psi\pi\pi}$ and ΔE distributions are fixed from the previous 2D fit to all events. Then we perform a binned minimum χ^2 fit to the $M_{K\pi}$ distribution using $K^*(892)^0$ and $(K^+\pi^-)_{\text{NR}}$ components, which are histogram PDFs obtained from MC samples. Note that the $B^0 \rightarrow X(3872)K_2^*(1430)^0$ decay is kinematically suppressed. The resulting fit result is shown in Fig. 2(a). We obtain 38 ± 14 (82 ± 21) signal events for the $B^0 \rightarrow X(3872)K^*(892)^0$ ($B^0 \rightarrow X(3872)(K^+\pi^-)_{\text{NR}}$) decay mode. This corresponds to a 3.0σ significance (including systematic uncertainties related to the signal yield) for the $B^0 \rightarrow X(3872)(\rightarrow J/\psi\pi^+\pi^-)K^*(892)^0$ decay mode, and a product of branching fractions of $\mathcal{B}(B^0 \rightarrow X(3872)K^*(892)^0) \times \mathcal{B}(X(3872) \rightarrow J/\psi\pi^+\pi^-) = (4.0 \pm 1.5(\text{stat.}) \pm 0.3(\text{syst.})) \times 10^{-6}$. The ratio of branching fractions is:

$$\frac{\mathcal{B}(B^0 \rightarrow X(3872)K^*(892)^0) \times \mathcal{B}(K^*(892)^0 \rightarrow K^+\pi^-)}{\mathcal{B}(B^0 \rightarrow X(3872)K^+\pi^-)} = 0.34 \pm 0.09(\text{stat.}) \pm 0.02(\text{syst.}). \quad (1)$$

In the above ratio, all systematic uncertainties cancel except those from the PDF model, fit bias and efficiency variation over the Dalitz distribution.

The same procedure is also applied to the $B^0 \rightarrow \psi'K^+\pi^-$ mode. With the sufficient yield, we use 51-MeV wide bins of $M_{K\pi}$ in the range $[0.600, 1.569]$ GeV/ c^2 . We perform a binned minimum χ^2 fit to the obtained $M_{K\pi}$ signal distribution again to extract the contributions of the $K\pi$ non-resonant and resonant components. For this purpose, we use histogram PDFs obtained from MC samples of several possible components of the $(K^+\pi^-)$ system: $K^*(892)^0$, $K_2^*(1430)^0$ and non-resonant $K^+\pi^-$ ($(K^+\pi^-)_{\text{NR}}$). The fit result is shown in Fig. 2(b). The $K^*(892)^0$ component dominates and we measure $\mathcal{B}(B^0 \rightarrow \psi'K^*(892)^0) = (5.88 \pm 0.18(\text{stat.})) \times 10^{-4}$, which is consistent with the world average [3].

In contrast to $B^0 \rightarrow \psi'(K^+\pi^-)$ (where the ratio of branching fractions is $0.68 \pm 0.01(\text{stat.})$), $B^0 \rightarrow X(3872)K^*(892)^0$ is not dominating in the $B^0 \rightarrow X(3872)K^+\pi^-$ decay mode.

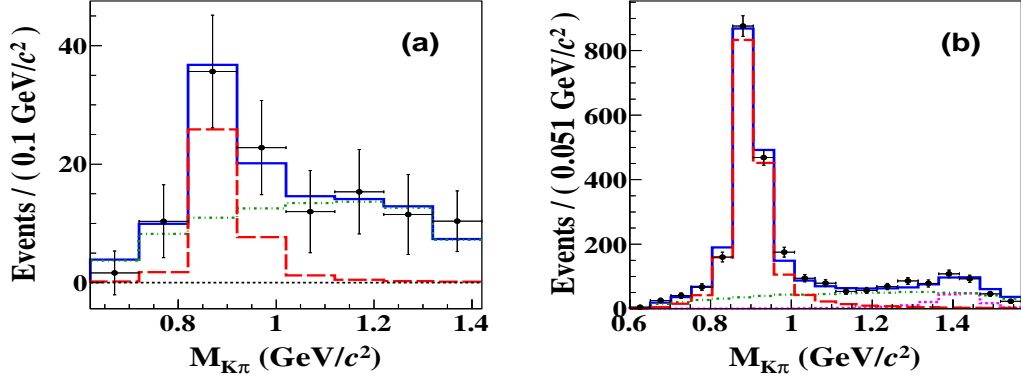


Figure 2: Fit to the background-subtracted $M_{K\pi}$ distribution: (a) for the $B^0 \rightarrow X(3872)(K^+\pi^-)$ decay mode, the curves show the $B^0 \rightarrow X(3872)K^*(892)^0$ [red long-dashed], $B^0 \rightarrow X(3872)(K^+\pi^-)_{NR}$ [green dot-dashed], as well as the overall fit [blue solid]. (b) for the $B^0 \rightarrow \psi'(K^+\pi^-)$ decay mode, the curves show the $B^0 \rightarrow \psi'K^*(892)^0$ [red long-dashed], $B^0 \rightarrow \psi'(K^+\pi^-)_{NR}$ [green dot-dashed], $B^0 \rightarrow \psi'K_2^*(1430)^0$ [magenta dashed] as well as the overall fit [blue solid],

We also investigate the decays $B^+ \rightarrow X(3872)(\rightarrow J/\psi\pi^+\pi^-)(K^0\pi^+)$. We perform a 2D fit to ΔE and $M_{J/\psi\pi\pi}$, as before. The projections of the 2D fit for $B^+ \rightarrow X(3872)(\rightarrow J/\psi\pi^+\pi^-)(K^0\pi^+)$ in the signal-enhanced regions are shown in Figs. 3(a) and (b). We find 35 ± 10 events for the $B^+ \rightarrow X(3872)(\rightarrow J/\psi\pi^+\pi^-)(K^0\pi^+)$ decay mode, corresponding to a 3.7σ significance (including systematic uncertainties). The product of branching fractions is $\mathcal{B}(B^+ \rightarrow X(3872)K^0\pi^+) \times \mathcal{B}(X(3872) \rightarrow J/\psi\pi^+\pi^-) = (10.6 \pm 3.0(\text{stat.}) \pm 0.9(\text{syst.})) \times 10^{-6}$. The above fit is validated for the ψ' mass region. The projections of the 2D fit for $B^+ \rightarrow \psi'(\rightarrow J/\psi\pi^+\pi^-)(K^0\pi^+)$ in the signal-enhanced regions are shown in Figs. 3(c) and (d). The branching fraction for $B^+ \rightarrow \psi'(\rightarrow J/\psi\pi^+\pi^-)(K^0\pi^+)$ is $(6.00 \pm 0.28(\text{stat.})) \times 10^{-4}$, while the world average of this quantity is $(5.88 \pm 0.34) \times 10^{-4}$.

Systematic uncertainties are summarized in Table 2. All systematic uncertainties are added in quadrature to give total systematic uncertainty of 5.4%, 8.0%, 7.0% for $B^0 \rightarrow X(3872)K^+\pi^-$, $B^+ \rightarrow X(3872)K_S^0\pi^+$ and $B^0 \rightarrow X(3872)K^*(892)^0$, respectively.

In summary, we report the first observation of the $X(3872)$ in the decay $B^0 \rightarrow X(3872)K^+\pi^-$, $X(3872) \rightarrow J/\psi\pi^+\pi^-$. The result for the $X(3872)$, where $B^0 \rightarrow X(3872)K^*(892)^0$ does not dominate the $B^0 \rightarrow X(3872)(K^+\pi^-)$ decay, is in marked contrast to the ψ' case. We have checked for a structure in the $X(3872)\pi$ and $X(3872)K$ invariant masses and found no evident peaks. We measure $\mathcal{B}(B^0 \rightarrow X(3872)(K^+\pi^-)) \times \mathcal{B}(X(3872) \rightarrow J/\psi\pi^+\pi^-) = (7.9 \pm 1.3(\text{stat.}) \pm 0.4(\text{syst.})) \times 10^{-6}$

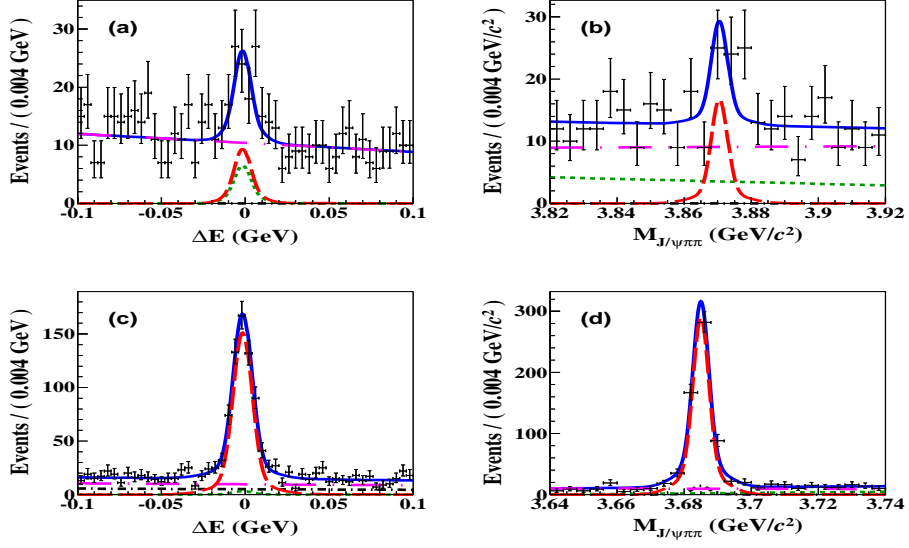


Figure 3: Projections of (a) ΔE distribution with $3.859 \text{ GeV}/c^2 < M_{J/\psi\pi\pi} < 3.882 \text{ GeV}/c^2$ and (b) $M_{J/\psi\pi\pi}$ distribution with $-11 \text{ MeV} < \Delta E < 9 \text{ MeV}$, (c) ΔE distribution with $3.675 \text{ GeV}/c^2 < M_{J/\psi\pi\pi} < 3.695 \text{ GeV}/c^2$, (d) $M_{J/\psi\pi\pi}$ distribution with $-11 \text{ MeV} < \Delta E < 9 \text{ MeV}$ for the $B^\pm \rightarrow X(3872)(\rightarrow J/\psi\pi^+\pi^-)K_S^0\pi^\pm$ decay mode (top) and for the $B^\pm \rightarrow \psi'(\rightarrow J/\psi\pi^+\pi^-)K_S^0\pi^\pm$ decay mode (bottom). Color representation is same as that of neutral mode.

Source	$X(3872)$ $K^+\pi^-$	$X(3872)$ $K^0\pi^+$
Lepton ID	3.4	3.4
Kaon ID	1.1	1.1
Pion ID	2.5	3.2
PDF modeling	+1.8	+4.2
Tracking efficiency	-1.3	-4.9
K_S^0 reconstruction	...	0.7
$N_{B\bar{B}}$	1.4	1.4
Secondary \mathcal{B}	0.4	0.4
Efficiency	0.6	1.0
Fit bias	0.6	3.1
Total	5.4	8.0

(a)

Source	$X(3872)K^*(892)^0$
Lepton ID	3.4
Kaon ID	1.1
Pion ID	2.6
PDF modeling	+1.5
Tracking efficiency	-1.4
Tracking efficiency	2.1
$N_{B\bar{B}}$	1.4
Secondary \mathcal{B}	0.4
MC statistics	0.2
Fit bias	4.6
Total	7.0

(b)

Table 2: Summary of the systematic uncertainties in percent (a) used for 2D fit. (b) used for the $M_{K\pi}$ background-subtracted fit in $B^0 \rightarrow X(3872)K^+\pi^-$.

and $\mathcal{B}(B^+ \rightarrow X(3872)K^0\pi^+) \times \mathcal{B}(X(3872) \rightarrow J/\psi\pi^+\pi^-) = (10.6 \pm 3.0(\text{stat.}) \pm 0.9(\text{syst.})) \times 10^{-6}$.

References

- [1] S.K. Choi *et al.* (Belle Collaboration), Phys. Rev. Lett. **91**, 262001 (2003).
- [2] Charge-conjugate decays are included unless explicitly stated otherwise.
- [3] K.A. Olive *et al.* (Particle Data Group), Chin. Phys. C, **38**, 090001 (2014).
- [4] S.K. Choi *et al.* (Belle Collaboration), Phys. Rev. D **84**, 052004 (2011).
- [5] R. Aaij *et al.* (LHCb Collaboration), Phys. Rev. Lett. **110**, 222001 (2013).
- [6] V. Bhardwaj *et al.* (Belle Collaboration), Phys. Rev. Lett. **107**, 091803 (2011).
- [7] R. Aaij *et al.* (LHCb Collaboration), Nucl. Phys. B **886**, 665 (2014).
- [8] P. del Amo Sanchez *et al.* (BaBar Collaboration), Phys. Rev. D **82**, 011101(R) (2010).
- [9] T. Aushev *et al.* (Belle Collaboration), Phys. Rev. D **81**, 031103(R) (2010).
- [10] B. Aubert *et al.* (BaBar Collaboration), Phys. Rev. D **77**, 011102(R) (2008).
- [11] A. Abashian *et al.* (Belle Collaboration), Nucl. Instrum. Meth. A **479**, 117 (2002); also see detector section in J. Brodzicka *et al.*, Prog. Theor. Exp. Phys. **2012**, 04D001 (2012).
- [12] S. Kurokawa and E. Kikutani, Nucl. Instrum. Meth. A **499**, 1 (2003), and other papers included in this volume; T. Abe *et al.*, Prog. Theor. Exp. Phys. **2013**, 03A001 (2013) and following articles up to 03A011.
- [13] D.J. Lange, Nucl. Instrum. Methods Phys. Res., Sect. A **462**, 152 (2001).
- [14] E. Barberio and Z. Wąs, Comput. Phys. Commun. **79**, 291 (1994); P. Golonka and Z. Wąs, Eur. Phys. J. C **45**, 97 (2006); **50**, 53 (2007).
- [15] R. Brun *et al.*, GEANT3.21, CERN Report DD/EE/84-1 (1984).
- [16] G.C. Fox and S. Wolfram, Phys. Rev. Lett. **41**, 1581 (1978).
- [17] A. Bala *et al.*, Phys. Rev. D **91**, 051101(R) (2015).
- [18] T. Skwarnicki, Ph.D Thesis, Institute for Nuclear Physics, Krakow 1986; DESY Internal Report, DESY F31-86-02 (1986).
- [19] K. Chilikin *et al.* (Belle Collaboration), Phys. Rev. D **88**, 074026 (2013).